

Chapter 11

Tailoring Performance of Polymer Electrolytes Through Formulation Design

Wei Wang, Dmitry Bedrov and Paschalis Alexandridis

Abstract The flammable organic solvent-based electrolytes used in lithium batteries impose serious safety concerns and temperature restrictions. A switch to solid polymer electrolytes can significantly increase chemical/mechanical stability, improve safety, reduce cost, and advance manufacturability, if only issues such as low conductivity and transference, limited operating temperature range, and insufficient mechanical strength can be overcome. To this end, significant research efforts have been directed to understand the mechanism of lithium ion motion in polymer matrices and to modify the chemistry, architecture, and morphology of the poly(ethylene oxide) polymer typically used in polymer electrolytes. Furthermore, the incorporation of nanoparticles into polymer electrolytes has created new opportunities for simultaneous improvement of conductivity and of mechanical properties. The performance of such composite polymer electrolytes can be modulated by the judicious surface chemical modification of the nanoparticles and/or by the addition of organic solvents or ionic liquids. The examples highlighted here point to the importance of formulation design for the improvement of the performance characteristics of multi-component systems such as polymer electrolytes.

W. Wang · P. Alexandridis (✉)

Department of Chemical and Biological Engineering, University at Buffalo,
The State University of New York (SUNY), Buffalo, NY 14260-4200, USA
e-mail: palexand@buffalo.edu

W. Wang

e-mail: wwang23@buffalo.edu

D. Bedrov

Department of Materials Science and Engineering, University of Utah,
Salt Lake City, UT 84112-0063, USA
e-mail: d.bedrov@utah.edu

© Springer International Publishing AG 2017

Z. Lin et al. (eds.), *Polymer-Engineered Nanostructures for Advanced Energy Applications*, Engineering Materials and Processes,
DOI 10.1007/978-3-319-57003-7_11

11.1 Introduction

Polymer electrolytes are widely utilized in electrochemical devices such as lithium-ion batteries, fuel cells, and supercapacitors for energy storage and conversion [1–8]. In this chapter, we focus on different additives and their effects on polymer electrolyte performance for lithium-ion batteries. A battery is composed of two electrochemically active electrodes [9] separated by an ion-conductive, electronically insulating electrolyte medium [10]. Rechargeable batteries find widespread use because of their repeated charge and discharge capability [11].

The electrolyte is one of the critical components of the lithium-ion battery. It facilitates ion transport and blocks electron conduction between the two electrodes [12]. Desirable properties of electrolytes are: high ionic conductivity and cation mobility, low electronic conductivity, good mechanical strength, thermal and chemical stability, and interfacial contact with electrodes, and large electrochemical stability window [13, 14]. Organic solvent-based electrolytes and ionic liquid-based electrolytes are two classes of electrolytes that have been well studied but they exhibit several drawbacks [15]. Organic solvent-based electrolytes have problems that include intrinsically poor cycling efficiency and flammability [16]. For ionic liquid-based electrolytes, a challenge is their relatively high viscosity which limits the attainable ionic conductivity [17–19]. Polymer electrolytes [20, 21] have thus been considered with an aim to overcome such limitations. The archetype polymer electrolyte is based on poly(ethylene oxide) (PEO) with lithium salt dissolved in it [22]. However, the semi-crystalline structure of PEO presents inherent problems as a polymer matrix for Li^+ : (1) not sufficiently high ionic conductivity, especially in ambient temperature; (2) insufficient mechanical strength; and (3) dendrite growth at the interface between electrode and electrolyte, which might cause internal short circuits [2].

In order to overcome these limitations of polymer electrolytes, several avenues have been explored. One promising line of investigation involves the introduction of nano-sized additives, as shown in Fig. 11.1 [23], in order to minimize the concentration of PEO crystalline domains without diminishing the PEO flexibility and mechanical stability over a wide temperature range [24, 25]. Inert oxide ceramics are the most common additives [26]. The effects of such additives have been analyzed in terms of Lewis acid–base interactions [24] between the surface groups of the fillers and active sites on the polymer chains.

Even though ternary systems incorporating nano-additives are promising, e.g., due to simultaneous improvement of conductivity and mechanical strength [24–27], composite polymer electrolytes (CPEs) are still away from desirable performance, e.g., room temperature conductivity higher than 10^{-3} S/cm [28]. For applications in electrochemical devices such as lithium-ion batteries [4, 12], research on CPEs is directed toward the formulation of modified ternary (polymer + lithium salt + nanoparticle) systems.

Different schemes have been reported for modifying each component in CPEs. Here, we focus on two avenues of modification: (1) surface chemical modification

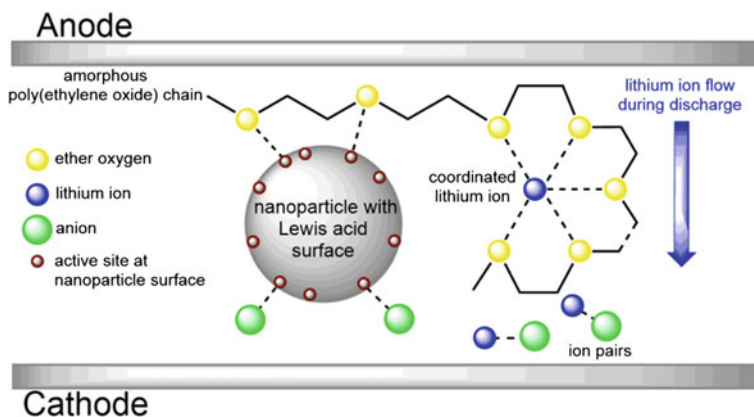


Fig. 11.1 Schematic of composite polymer electrolytes in the context of lithium-ion batteries

of nanoparticles, e.g., functionalization by oligomer groups or by ionic liquids; (2) physical modification via the addition of components such as organic solvents or ionic liquids. Section 11.2 discusses Li^+ transport mechanisms and factors that affect it in polymer-based electrolytes. Section 11.3 addresses the effect of nanoparticles on CPE properties and performance. Section 11.4 discusses nanoparticle chemical modification. Section 11.5 is concerned with the physical addition of a fourth component to CPEs. The purpose of Sects. 11.4 and 11.5 is to exemplify how different formulation modifications of CPEs have been designed and implemented, and to inspire ideas on novel CPE design for further CPE performance improvement.

11.2 Polymer-Based Electrolytes

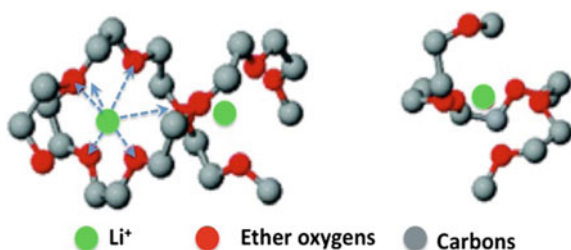
First, we review key molecular mechanisms and phenomena influencing the motion of Li ions (and their counter-ions) in a polymer matrix, and we outline several major challenges that conventional polymer electrolytes are facing to become an efficient alternative to conventional organic solvent electrolytes. We use PEO-based polymer electrolytes to illustrate these issues as the overwhelming majority of polymer electrolytes investigated to date are PEO-based. In addition to a large number of experimental studies, PEO-based electrolytes have also been studied by molecular simulation [29–41], and therefore these systems provide good case studies to illustrate the full complexity of understanding and design of efficient polymer electrolytes.

11.2.1 Mechanism of Li^+ Motion in PEO-Based Polymer Electrolytes

PEO is the quintessential polymer electrolyte owing largely to its effectiveness at dissolving lithium salts due to strong Li^+ -ether oxygen binding. Quantum chemistry (QC) and molecular dynamics (MD) simulation studies [29, 42] of PEO have revealed that Li^+ cations are very strongly coordinated by an average of six ether oxygen atoms as shown in Fig. 11.2. Coordination of Li^+ usually involves a single PEO chain, with occasional coordination by two polymer chains.

The nature of ether– Li^+ interactions strongly affects the mechanism of Li^+ mobility in PEO-based solid polymer electrolytes (SPEs). This can be understood by comparing the mechanism of Li^+ diffusion in oligoethers with that in organic solvents. Li^+ motion in organic liquid electrolytes (typically carbonates) occurs by a combination of vehicular (with a solvent shell) and structural (exchange of solvent shell) diffusion [43]. In contrast, simulations reveal that Li^+ diffusion in pentaglyme + $\text{Li}[\text{bis}(\text{trifluoromethyl}) \text{ sulfonyl}] \text{imide}$ (TFSI) [43] salt occurs entirely by a vehicular mechanism, i.e., a pentaglyme/ Li^+ complex diffuses long distances before Li^+ exchanges between complexing molecules. The residence time of Li^+ with a pentaglyme is around 50 ns, compared to ~ 1 ns in carbonate, or 3–10 ns in ionic liquids [44]. While the lack of an efficient structural diffusion mechanism has relatively little influence on Li^+ motion in pentaglyme because of the fast center-of-mass diffusion of the low molecular weight (MW) solvent, the situation is different in higher molecular weight (MW) PEO. Because the center-of-mass diffusion of PEO is negligible, a Li^+ cation must change coordinating PEO chains, i.e., it will undergo “jumps” between PEO chains [45]. Compared with pentaglyme, Li^+ transport is considerably slower in the PEO-based SPE, while the diffusion of TFSI is reduced relatively little, indicative of the relative independence of anion motion from that of the polymer. This leads to a significantly lower transference number in the polymer electrolyte as a much greater fraction of charge is carried by the anion due to the very slow Li^+ motion. Furthermore, the PEO chain center-of-mass motion is considerably slower than that of the cation, intimating that the vehicular mechanism, which is so important in the oligoethers, does not contribute significantly to Li^+ motion in the SPE. Instead, Li^+ motion in the PEO-based electrolytes resembles diffusion along PEO chain contours with occasional inter-chain jumps on a time scale of ~ 100 ns [41].

Fig. 11.2 Representative configurations of Li^+ coordination by PEO



Simulation [29] and experimental studies [46, 47] of linear PEO-based electrolytes also showed strong dependence of the Li^+ and anion motion on salt concentration. While the anion motion remains much faster than that of Li^+ for all salt concentrations, the translational dynamics of both ions decrease dramatically with increasing salt concentration, suggesting strong coupling with local polymer relaxations. The slowing of polymer segmental dynamics with increasing salt content is due to the strong binding between ether oxygens and Li^+ , which greatly restricts conformational motion. As a result, a maximum in PEO-based electrolyte conductivity is observed for Li:EO molar ratio $\sim 1:10$ due to two counter-acting effects: Ionic conductivity increases with increasing salt concentration due to the increase in the number of charge carriers, while increasing salt concentration slows down polymer dynamics, thereby decreasing also the Li^+ transport [29, 48].

11.2.2 Influence of Polymer Architecture

Polyethers of comb-branch chain architecture have been investigated in efforts to develop polymer electrolytes that take advantage of the ability of oligoethers to coordinate Li^+ while, at the same time, preventing crystallinity due to use of short side chains, and allow for separate optimization of the backbone properties from those of the side chains [49]. The ideal comb-branch electrolyte might, for example, use a glassy backbone polymer, thereby leading to good mechanical properties, while Li^+ transport would be carried out by flexible ether (PEO) side chains (Fig. 11.3a). The use of relatively short side chains not only reduces/prevents PEO crystallinity, but may also facilitate the inter-chain hopping needed for large-scale Li^+ transport, due to sharing of Li^+ cations between side chains. Several polymer electrolytes formed from comb-branch polymer have been studied experimentally [50, 51] and in simulations [30], however, studies showed that the conductivity of the comb-branch electrolytes is very similar to that of the linear PEO electrolytes. Molecular simulations of the comb-branched systems revealed that Li^+ motion occurs primarily by hopping of the cation from one side chain to another [30]. However, a fraction of Li^+ cations are partially coordinated by the polyether backbone and, therefore, have very slow dynamics and do not contribute to conductivity. The slow dynamics of cations that are partially coordinated by the chain backbone can be correlated with conformational transitions of PEO segments: those that are closer to the backbone are significantly slower due to steric crowding. Hence, the Li^+ complexed by the slower segments exhibits the lowest mobility. Therefore, while the comb-branched PEO-based electrolytes investigated so far did not show improved Li^+ conductivity, they provided evidence of two promising trends: (1) the Li^+ that is not complexed by the backbone exhibits higher mobility than in the linear PEO electrolyte, indicating that the short side chains do promote inter-chain hopping, and (2) the Li^+ mobility, at least for those cations not complexed by the polymer backbone, is largely independent of the backbone motion.

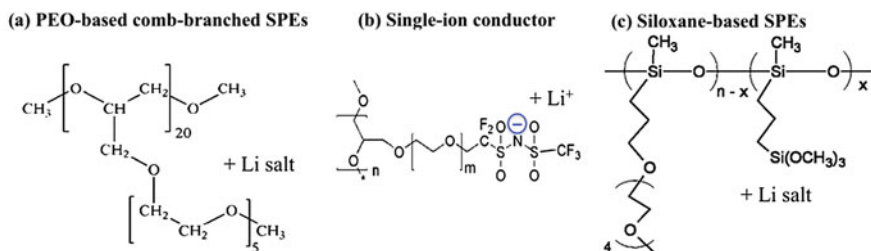


Fig. 11.3 Representative PEO-based polymer architectures considered for SPEs

One disadvantage of current PEO-based electrolytes is their low transference number due to relatively high anion mobility. Large-scale anion motion in comb-branch electrolyte can be eliminated by attaching the anions to the polymer (Fig. 11.3b), however, this has a deleterious effect on Li^+ mobility [52], because anions play an important role in the ability of Li^+ cations to undergo inter-chain jumps. While attaching the anion to the polymer has the advantage of improving transference number (all charge is carried by Li^+), further reducing the Li^+ mobility is a major disadvantage. Addition of a solvent/plasticizer [e.g., ethylene carbonate (EC)] to the single-ion conductor electrolytes showed dramatic improvement in ionic conductivity over the non-plasticized single-ion conductor. EC increases the rate of polymer conformational transitions, yet it is not directly involved in coordination and transport of Li^+ [53]. An experimental investigation [54] of a single-ion conductor made from blending PEO with a comb-branch polystyrene-based polyanion showed a low conductivity, but depending dramatically upon the polyanion structure. Such blending provides additional degrees of freedom in terms of composition and architecture design of polymer electrolyte [55].

Finally, there has been an interest in siloxane as a component for polymer electrolytes due to its conformational flexibility (and hence low glass transition temperature) and electrochemical stability. Because siloxane itself has limited ability to solvate Li^+ , siloxane-based electrolytes contain ether groups for the purpose of solvating and transporting Li^+ . Siloxane-ether oligomers [56–59] and comb-branch polymers with siloxane backbones and PEO side chains [60–63] (Fig. 11.3c) show indeed improved conductivity. However, these electrolytes do not exhibit adequate room temperature conductivity and mechanical stability for most applications.

11.2.3 Influence of Polymer Morphology

Microphase-separated copolymers consisting of PEO covalently linked to a different type polymer offer an attractive avenue to achieving both high ionic

conductivity and dimensional stability in polymer electrolytes [64]. Microphase-separated copolymers can also prevent the formation of semi-crystalline spherulites that reduce contact with electrodes [65]. It is important to note that added lithium salts modulate the degree of block segregation and can alter the resulting polymer organization and properties emanating from this [66, 67]. Copolymer electrolytes that provide nano-scale domains ion-rich and ion-lean can be advantageous [68]. The ion-rich domains play a primary role in ion transport and, to this end, the polymer segments localized there should be mobile, through appropriate polymer chemistry and architecture, or through heating and/or the introduction of plasticizers. The polymer segments of the ion-lean domains can be designed such that they contribute to the mechanical rigidity of the polymer electrolyte [69].

The conductivity of heterogeneous polymer electrolytes involves a pre-factor f (≤ 1) that accounts for the tortuosity and connectivity of the conducting domains [68]. In the case of block copolymer electrolytes [69] with well-defined nano-scale morphologies [70], an ideal morphology factor, f_{ideal} , can be defined based on perfectly ordered lamellae, cylinders, etc. [68]. Experimentally determined f of heterogeneous polymer electrolytes relevant to Li-ion batteries is typically lower than f_{ideal} [67] indicating the importance of the resistance at grain boundaries, and associated with it, the importance of processing history [71, 72].

The effects of morphology on the ionic conductivities of polymer electrolytes are significant [69]. A polymer electrolyte membrane of a typical 100 μm thickness encompasses several micro-scale grains, each with well-defined nano-scale organization of the polymer, but each with different orientation. For intra-grain ion transport, the continuity and connectivity of the ion-conductive nano-scale domains are important, whereas for inter-grain ion transport, the connectivity of conducting channels across the boundary between adjacent grains is important. The mesoscopic and macroscopic orientation/alignment of nano-structured domains are outstanding issues in the field of microphase-separated polymers, but several methodologies have been found effective, such as thermal or solvent annealing, epitaxy, templating, stretching, shear alignment, application magnetic or electric fields, or combinations thereof [72–83].

While nano-scale polymer organization is driven by thermodynamics, meso-scale grain size and alignment are typically an outcome of processing, either deliberate or unintended consequence of sample preparation and testing [84]. An investigation of thermal history on the ionic conductivity of LiTFSI (lithium bis(trifluoromethanesulfonyl)imide, $\text{LiN}(\text{SO}_2\text{CF}_3)_2$)-doped PEO-PS (polystyrene) block copolymer electrolytes showed the conductivity of low MW samples to decrease after annealing, while the conductivity of high MW samples was unaffected. This was attributed to the development of well-defined nanostructure in the annealed samples [85]. A subsequent study on the dependence of ionic conductivity on the grain size of a lamellar PEO-PS block copolymer electrolyte showed well-formed lamellar grains to be less conducting than poorly defined, small grains [86]. Well-ordered solvent-cast films of polymerized ionic liquid block copolymers (single-ion conductors) exhibited up to an order of magnitude higher conductivity than poorly ordered melt-pressed films [87].

11.3 Composite Polymer Electrolytes

As nanoparticles are incorporated into a PEO + salt electrolyte to form a composite polymer electrolyte (CPE) [24, 25], the concentration of PEO crystalline domains can be reduced without harming the PEO chain flexibility. This is a main reason for the observed ionic conductivity enhancement in CPEs. Moreover, the cation transference number (t^+ , fraction of the current carried by lithium ions) and the mechanical strength can be improved simultaneously over a wide temperature range. These effects of nanoparticles on polymer electrolytes are highlighted in this section.

11.3.1 Nanoparticle Effects on Conduction and Transference

The most critical requirement for the application of polymer electrolytes in lithium-ion batteries is the ionic conductivity. This is commonly described by the Vogel–Tamman–Fulcher (VTF) equation [25, 88, 89].

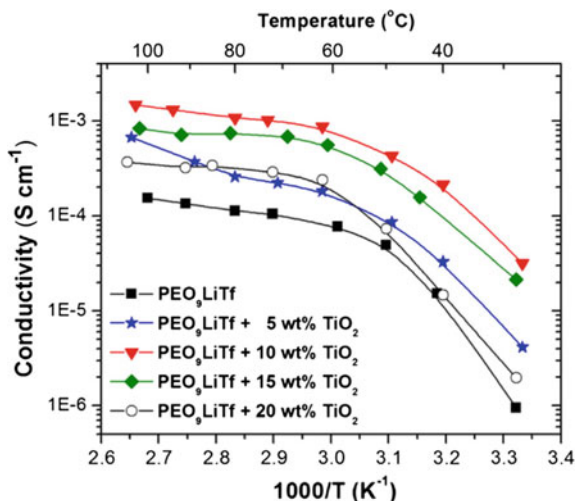
$$\sigma = AT^{-1/2} \exp[-E_a/(T - T_0)] \quad (11.1)$$

The conductivity variation with inverse temperature for the CPEs PEO (4×10^6 g/mol)–LiTf (lithium trifluoromethanesulfonate or lithium triflate, LiCF_3SO_3 , EO: $\text{Li}^+ = 9$)– x wt% TiO_2 ($x = 0, 5, 10, 15$ and 20) is shown in Fig. 11.4. Only the 5 wt% sample behaves differently compared to the typical VTF behavior of other electrolytes. Specifically, the conductivity increases faster at temperatures $T > 80$ °C due to the increased mobility of ions via Lewis acid–base interaction. The sample with 10 wt% TiO_2 exhibited the optimal ionic conductivity among those studied. Further addition of nanoparticles (20 wt%) led to a drop in conductivity because of nanoparticle agglomeration that hindered ion transport [90].

In addition to their effect on ionic conductivity, nanoparticles also affect the transference number (t^+) of CPEs. t^+ directly describes the charge transport and thus the current of a specific ion [91]. Specifically, t^+ indicates the fraction of the current that is carried by the cation (Li^+) in the electrolytes. It is desirable to achieve a high t^+ value in order to enhance the electrode reaction kinetics and to eliminate the concentration gradients within the battery so that the internal voltage drop could be lowered and the output current increased [92]. t^+ is most commonly calculated by Eq. (11.2) [93, 94].

$$t^+ = \frac{\mu^+}{\mu^+ + \mu^-} = \frac{D^+}{D^+ + D^-} \quad (11.2)$$

Fig. 11.4 Variation of conductivity with inverse temperature on the heating run for composite polymer electrolytes incorporating TiO₂ ceramic powder; PEO (4 × 10⁶ g/mol)–LiTf (EO:Li⁺ = 9)–*x* wt% TiO₂ (*x* = 0, 5, 10, 15 and 20) (Reproduced from Ref. [90] with kind permission of © 2014 Elsevier)



In Eq. (11.2), D^+ and D^- are the cation and anion self-diffusion coefficients; μ^+ and μ^- are the mobility [95, 96] of the cation and anion, respectively.

High lithium transference number (t_{Li^+}) at ambient temperature contributes to efficient battery performance [97, 98]. In view of the importance of t^+ , the effect of additive surface functional sites on the transference number (t^+) is discussed here. For the system PEO–LiCF₃SO₃ (EO:Li⁺ = 20)–10 wt% Al₂O₃ (basic, neutral, or acidic, $d = 5.8$ nm), the transference number t^+ increased in the sequence of undoped ($t^+ = 0.46$) < basic Al₂O₃ ($t^+ = 0.48$) < neutral Al₂O₃ ($t^+ = 0.54$) < acidic Al₂O₃ ($t^+ = 0.63$) [99]. As for an explanation, the hydrogens of acidic ceramic surfaces (Lewis acid) form hydrogen bonds with the lithium salt anions and the ether oxygens (Lewis base) [99], which promote salt dissociation and also decrease the PEO crystallinity [98, 99]. In this way, t^+ increased. As for the neutral and basic Al₂O₃, the number of Lewis acid sites decreased, leading to a weaker increase in t^+ . This discussion would be more interesting if the number of acidic sites on the surface could be quantified in combination with oxygen vacancy analysis. The efficiency of acidic sites on the t^+ increase would thus be revealed.

We discuss above factors affecting the lithium transference number t^+ . But how is t^+ related to conductivity? Conductivity and t_{Li^+} results have been compared for CPEs, with the additive being ionically active or inert SiO₂ particles (active SiO₂ was mesoporous silica MCM-41 absorbing plasticizers of ethylene carbonate (EC)/propylene carbonate; inert SiO₂ was mesoporous silica MCM-41 without plasticizers). For PEO (300,000 g/mol)–LiClO₄ (EO:Li⁺ = 16)–SiO₂ (1000 m² g⁻¹), the conductivity initially increased upon addition of active SiO₂, attained a maximum value of about 2.4×10^{-5} S cm⁻¹ at 10 wt% active SBA-15 (even though the free Li ion percentage was optimized at 5 wt%), followed by a mild decline with further loading of active SBA-15 [92]. In parallel, the transference number t^+ increased from 0.42 for the undoped sample, reached a maximum value of 0.54 at 10 wt%

active SBA-15, followed by a drastic decline with further loading of active SBA-15 (Fig. 11.5). As for the reasons, the $-OH$ groups on the surface of SBA-15 compete with Li^+ (both as Lewis acid) to interact with ether oxygens and ClO_4^- (both as Lewis base) to promote Li^+ transport and thus enhance t^+ . When the additive content exceeded 10 wt%, nanoparticle aggregation drastically impaired the Li^+ transference number.

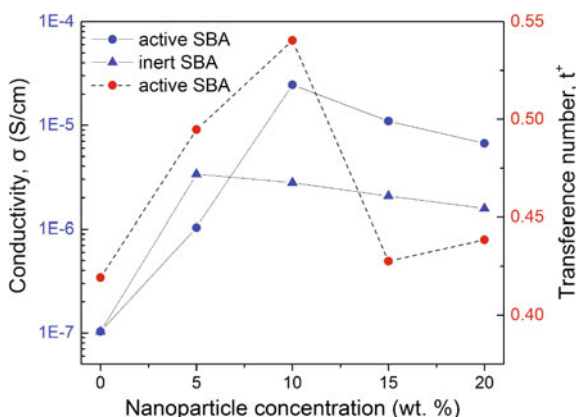
In another study, mSBA-15 (silane-functionalized silica of SBA-15, $1000 \text{ m}^2 \text{ g}^{-1}$) was added into PEO ($300,000 \text{ g/mol}$)– $LiClO_4$ (EO: Li^+ = 16). The ionic conductivity (σ) and t^+ presented a similar increasing trend and achieved their peak values simultaneously at a level of 5 wt% doping. This mSBA-15 additive has been proposed to promote lithium salt dissociation and produce more free lithium ion, and to lower the activation for ion transport [100]. Following the peak values, σ decreased gradually and t^+ decreased steeper upon further nanoparticle addition.

11.3.2 Nanoparticle Effects on Mechanical Properties

Polymer electrolytes are promising to avoid drawbacks of the liquid-state electrolytes and help to expand the operating conditions, even in harsh conditions, e.g., high temperature. However, the mechanical strength of neat PEO is not satisfactory, especially at a high working temperature due to its low-melting temperature $66\text{--}75 \text{ }^\circ\text{C}$. The binary systems of PEO with lithium salt do not exhibit an obvious improvement of mechanical strength despite the transient crosslinks [101] formed between lithium ions and ether oxygens. Thus, the mechanical properties of polymer electrolytes with nano-additives became of interest. In this section, we discuss how nanoparticles can improve CPE mechanical properties such as tensile strength, yield strength, elastic and viscous modulus.

Silane (KH550)-modified silica was added for simultaneous enhancement of the ionic conductivity and mechanical strength of PEO ($MW = 300,000 \text{ g/mol}$)–

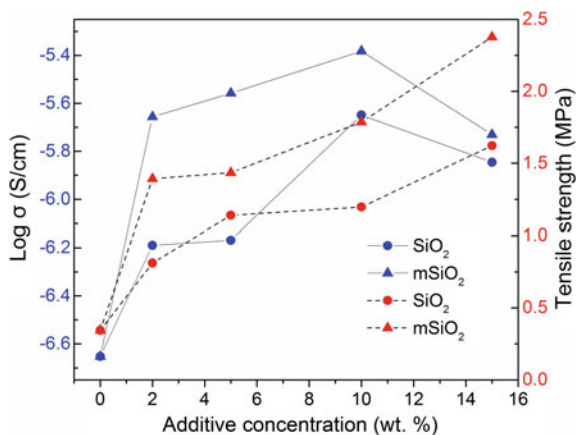
Fig. 11.5 Ionic conductivity σ and lithium transference number t^+ as a function of **a** active SBA-15 and **b** inert SBA-15 content for PEO ($300,000 \text{ g/mol}$)– $LiClO_4$ – SiO_2 ($1000 \text{ m}^2 \text{ g}^{-1}$) CPE at $25 \text{ }^\circ\text{C}$. *Solid lines* correspond to the Y axis on the left. The *dashed line* corresponds to the Y axis on the right (Data from Wang et al. Ref. [92])



LiClO_4 ($\text{EO}:\text{Li}^+ = 16$) [102]. Less than 10 wt% nanoparticles caused the formation of an amorphous interface region around the nanoparticles and an increase in the polymer amorphous fraction [103], which led to an increase of the ionic conductivity as shown in Fig. 11.6. Further addition (>10 wt%) of nanoparticles led to agglomeration that impaired the ionic conductivity. In contrast, the CPE tensile strength kept increasing upon addition of nanoparticles to 15 wt% [102].

In another study, the tensile modulus and yield strength of PEO (300,000 g/mol)– LiClO_4 –(mSBA-15: silane-functionalized mesoporous silica) increased with increasing mSBA-15 amount in the 0–15 wt% range [100]. This enhancement is due to the addition of ceramic fillers which acted as crosslinking media inside the polymer matrix by their surface interactions [104]. However, the enhancement was not always monotonic. For PEO (100,000 g/mol)– LiClO_4 –(montmorillonite–CNT), the optimized tensile strength was achieved upon 5 wt% clay–CNT incorporation into the hybrid. The tensile strength increased by 160% compared to the PEO electrolyte [105]. This reinforcement has been ascribed to the large aspect ratio and surface roughness of the clay–CNT hybrid filler, which lead to strong interactions between nano-fillers and polymer [105]. The different surface roughness may also explain the difference in the optimal nano-additive amount for maximized tensile strength between these two systems. In combination with the knowledge that the maximum conductivity occurred at 10 wt% nano-additive [92, 106, 107], the incorporation of 10 wt% nano-additive appears to offer an optimal combination of improved mechanical properties as well as optimized ion conductivity. Very likely, a CPE composition involving around 10 wt% additive would also correspond to minimized T_g , T_m , and crystallinity. Of course, the surface conditions, e.g., roughness, functionalization, and possible surface defects of the nanoparticle additives may cause the final result to deviate.

Fig. 11.6 Ionic conductivity and tensile strength for PEO (MW = 300,000 g/mol)– LiClO_4 ($\text{EO}:\text{Li}^+ = 16$) with various contents of SiO_2 and KH550-modified SiO_2 (m SiO_2) at 30 °C. *Solid lines* correspond to the Y axis on the *left*. *Dashed lines* correspond to the Y axis on the *right* (Data from Fan et al. [102])



11.4 Ternary Polymer Electrolytes

With an aim to further improve the CPE performance, Sect. 11.3 discusses the silica nanoparticle modification by plasticizers treatment or by silane compound to tune the interactions between polymer, nanoparticles, and Li^+ ions (the notion of tuning interactions also applies to the physical modification of CPEs that is discussed in Sect. 11.4). The compatibility of nanoparticles with the polymer matrix can be improved in this way. We discuss here pseudo-ternary systems consisting of polymer, salt, and surface-modified nanoparticles. Typical methods of nanoparticle chemical modification with polymers and ionic liquids are addressed in Sects. 11.4.1 and 11.4.2, respectively.

11.4.1 Polymer-Functionalized Nanoparticles

In order to improve the compatibility of nanoparticles with the polymer matrix for a better performance of CPEs, surface grafting of nanoparticles with oligomers (short chain polymers) that share the same repeating unit as the polymer matrix has been actively investigated. One example involves polyhedral oligomeric silsesquioxane (POSS) nanoparticles functionalized by poly(ethylene glycol) (PEG) [108, 109], and another example concerns silica functionalized by PEO [110]. POSS is an organic–inorganic hybrid compound typically formed by inorganic cubic core (siloxane cage) and outer organic groups (pendant arms), with a general formula of $(\text{RSiO}_{1.5})_n$, $n = 6, 8, \text{ or } 10$ [111]. POSS are of interest for their broad applications [73, 83], including in connection to CPEs [112–115].

Different ways of POSS [116–118] application in combination with ion-conductive polymers (e.g., PEO) for electrolytes in lithium-ion batteries have been reported [73, 108, 109, 111–118]. In the first case, the outer organic groups of POSS are ion-conductive PEO chains, and the organic–inorganic hybrid compound (generally denoted as POSS–PEO) itself acts as an electrolyte with the grafted PEO serving as conducting media. In this case, the POSS–PEO is the matrix. In the second case, POSS–PEO can also be used as an additive for binary PEO + salt polymer electrolytes; with the help of grafted PEO chains, compatibility with the PEO matrix can be improved. A comparison of these two cases is presented next.

For the first case of POSS–R as matrix, POSS–PEO₈ ($n = 4$, where n denotes the number of PEO-repeating units attached to POSS, while the subscript 8 of PEO denotes octa-functionalization on POSS) and PEO 600 K were compared as ion conduction medium upon addition of LiClO_4 at a fixed amount of $\text{EO}:\text{Li}^+ = 12$. As shown in Fig. 11.7a, the POSS–PEO₈ ($n = 4$)-based electrolyte exhibited higher conductivity than that of PEO (600 K)-based electrolyte over the whole temperature range. In contrast, in Fig. 11.7b, PEO (600 K)– LiClO_4 ($\text{O}:\text{Li} = 12:1$) exhibited an abrupt conductivity change [108] at the PEO-melting temperature of around 327 K. At low temperatures ($T < T_m$), neat POSS–PEO₈ ($n = 4$, $\text{O}:\text{Li} = 12:1$) presented a

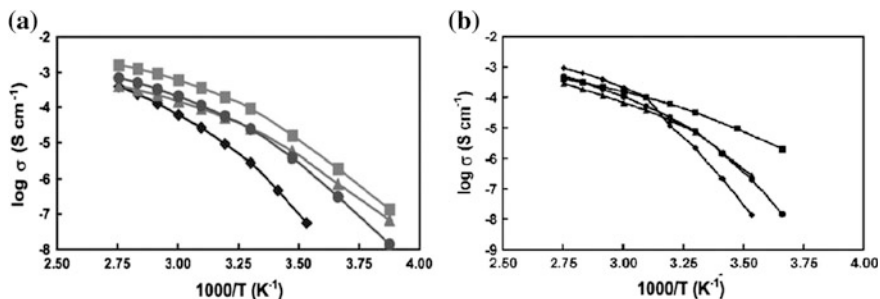


Fig. 11.7 **a** Conductivities of (i) POSS–PEO ($n = 3$)₈ (filled triangle); (ii) POSS–PEO ($n = \langle 8 \rangle$)₈ (filled circle); (iii) PEGDME (MW = 500 g/mol) (filled square); and PEO (MW = 600 K) (filled diamond). All samples are prepared using LiClO₄ with O/Li = 8:1. Reproduced from Ref. [109] with kind permission of © 2006 The Electrochemical Society; **b** conductivity plots of (i) POSS–PEO₈ ($n = 4$) (filled square); (ii) PEO (MW = 600 K) (filled diamond); (iii) blend of 50 wt% POSS–PEO₈ ($n = 4$) with 50% PEO (600 K) (filled triangle); and (iv) blend of 60 wt% POSS–PEO($n = 4$)₈ with 40 wt% PEO (600 K) (filled circle); all samples are prepared using LiClO₄ with O/Li = 12:1 (Reproduced from Ref. [108] with kind permission of © 2007 American Chemical Society)

higher conductivity than that of PEO (600 K)–LiClO₄ (O/Li = 12:1) because of the low viscosity of POSS–PEO₈ and the crystallization of PEO. At high temperatures ($T > T_m$), it is the opposite case because of the inert SiO_{1.5} core of POSS–PEO.

For the second case of POSS–R as additive, at low temperatures, the mixture of POSS–PEO₈ ($n = 4$) /PEO (600 K) exhibited a conductivity between that of POSS–PEO₈ ($n = 4$)- and PEO (600 K)-based electrolytes. This was attributed to the crystallinity decrease by addition of POSS–PEO₈ into PEO (600 K); at high temperatures, the mixture of POSS–PEO₈ ($n = 4$) /PEO (600 K) exhibited lower conductivity than PEO (600 K)–LiClO₄ (O/Li = 12:1) because of the presence of the inert SiO_{1.5} core [108].

Fumed silica (FS) ($d = 12$ nm, surface area = 200 m²/g) functionalized by non-polar alkyl moieties (FS-C₈) or by polar PEO oligomers with MW = 200 g/mol (FS-C3EG3ME) has been used in oligomer-based electrolytes with two different lithium salts, respectively: polyethylene glycol dimethyl ether (PEGDME, Mw = 250 g/mol)–LiN(CF₃SO₃)₂/LiCF₃SO₃ (Li:O = 1:20) [110]. The conductivity was not improved but rather dropped marginally with the addition of fumed silica at a doping amount of 10 and 20 wt%. FS-C3EG3ME even brought down the conductivity to a larger extent compared to FC-C8. High conductivities of over 10⁻³ S/cm at the 295–400 K temperature range were reported [110]. This high conductivity was attributed to the low molecular weight matrix of PEGDME with MW = 250 g/mol. In this case of low molecular weight oligomer electrolyte, the conductivity benefited from the liquid state of the matrix, while the addition of nanoparticles increased the viscosity to impair the ionic conductivity to some degree. This is opposite to the nanoparticle effect in SPEs to improve ion conduction. However, when it comes to a solid polymer matrix, it is possible that

FC-C3EG3ME would act more effectively to facilitate ion transport for its lithium ion coordination sites of EO units [114, 117]. Therefore, the incorporation of these differently grafted fumed silica into solid polymer electrolytes awaits to be investigated for comparison.

Other studies of polymer-functionalized nanoparticles include silica grafted with: [119] (1) homopolymer of poly(ethylene glycol) methyl ether methacrylate (PEGMA) of different molecular weight, or (2) poly(ethylene glycol) methyl ether methacrylate (PEGMA) copolymer, as additive for matrix of poly(ethylene glycol) dimethyl ether (PEGDME, $M_w = 500$ g/mol)–Li/I₂ (EO:Li = 10:1). This system was reported to achieve room temperature conductivity 10^{-4} S/cm, but this result was around a threefold decrease from the undoped binary samples [119]. Thus, it can be concluded that the effectiveness of modified nanoparticle on properties of CPEs differs depending on the liquid or solid state of the polymer matrix, and it is not always the case that chemically functionalized nanoparticles can help improve the performance of the electrolytes. Similar work has been published, e.g., PEO-grafted silica was used in the matrix of PEO/sulfoisophthalate ionomers to improve the room temperature ionic conductivity by an order of magnitude [120].

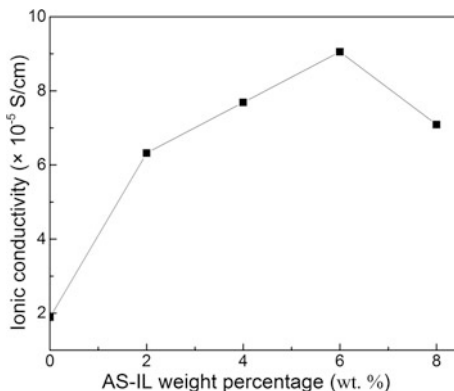
11.4.2 Ionic Liquid-Modified Nanoparticles

In addition to PEO oligomer grafting on POSS surfaces, ionic liquids have also been introduced for nanoparticle chemical functionalization. The application of ionic liquids in polymer electrolytes has been motivated by their good chemical and electrochemical stability, low flammability, and negligible vapor pressure [18, 121–126]. Researchers then considered nanoparticles and ionic liquids chemically combined together as additives for CPEs. For example, studies have been reported on 1-methyl-3-[(triethoxysilyl)propyl]imidazolium chloride (TMICl) tethered to TiO₂ nanoparticles (20 nm in size) used in electrolytes for dye-sensitized solar cells (DSSC) [127], and on 1-undecyltrimethoxysilane-3-butyl imidazolium bis(trifluoromethylsulfonyl) imide tethered to ZrO₂ (average particle size 86 ± 2 nm) as hybrid electrolytes for lithium-ion batteries [128].

In a recent study, 1-methyl-3-propyl-imidazolium bromide ionic liquid attached on silica (MPIm-AS or AS-IL, size not given) was reported to improve the ionic conductivity of PEO ($MW = 10^6$ g/mol)/poly(ethylene imine) (PEI, $MW = 1.2 \times 10^5$ g/mol)–LiClO₄ [129]. (PEO:PEI = 10:1, lithium salt, and nanoparticle amount not specified.) The novelties included: (1) physical mixing of PEI with PEO as polymer matrix, PEI itself providing alternative coordination sites to complex with lithium ions by its nitrogens on polymer chains; (2) blending with PEI makes the electrolyte formation easier due to its lower viscosity, and thus unnecessary to use plasticizers.

The impedance became much smaller upon the introduction of MPIm-AS, with the optimal content observed at 6 wt% and the corresponding conductivity at 9.1×10^{-5} S/cm as shown in Fig. 11.8 [129]. In contrast to the Sect. 11.3

Fig. 11.8 Ionic conductivity of poly(ethylene oxide) ($M_w = 10^6$ g/mol)/poly(ethylene imine) ($M_w = 1.2 \times 10^5$ g/mol)– LiClO_4 (PEO:PEI = 10:1) containing 0, 2, 4, 6, and 8 wt % of AS-IL at room temperature (Data from Kim et al. [129])



discussion of optimal doping at 10 wt%, [92, 106, 107], the optimal doping concentration of AS-IL is decreased in this case to 6 wt%. The difference may be due to the different composition of the polymer matrix. The different electron-donating ability of oxygen and nitrogen led to a different solvating ability for the lithium ions and interactions with AS-IL [129]. When the amount of AS-IL exceeded 6 wt%, particle aggregation hindered the ion transport and decreased the ionic conductivity.

Decreasing melting temperature T_m and heat of fusion ΔH_m values are reported in Table 11.1. It is worth noting that the optimal conductivity point, at 6 wt% MPIIm-AS, is not the point of lowest PEO crystallinity. This was explained by a greater amount of additive that aggregated and impaired the ion transport within the matrix [129].

Another report of this type concerns 1-methylimidazole chloride (ImCl) ionic liquid-tethered TiO_2 (size not provided) as additives for plasticized polymer electrolytes: PEO ($M_w = 10^6$ g/mol) /PMMA ($M_w = 1.2 \times 10^5$ g/mol)– LiClO_4 –propylene carbonate–(3–12 wt%) IL– TiO_2 [130]. This study also followed the idea of “tuning the recipe” for CPEs by blending polymers as co-matrix, and also by the addition of plasticizer. The maximum conductivity was 1.05×10^{-4} S/cm at 9 wt% IL– TiO_2 [130]. Further addition of IL– TiO_2 led to conductivity drop due to immiscibility or aggregation of IL– TiO_2 . For this type of IL-tethered nanoparticles, the topic of how the two counterparts, i.e., ionic liquid and nanoparticle, work in tandem with the CPEs remains of interest to this field.

To sum up Sect. 11.4, chemical modification of ternary CPEs is seeking to improve the compatibility of nanoparticles with the polymer matrix or to improve the “solubility” of the nano-additives in the polymer matrix. One common method is to graft functional groups onto the nanoparticle surface to interact with ether oxygens of the PEO matrix. Following the chemical modification of the nanoparticles, pre-existing Lewis acid–base interactions have been disturbed. The optimum doping (for optimal ionic conductivity) is no longer the typical 10 wt% for untreated nanoparticles [92, 106, 107]. For different studies, either the polymer matrix can accommodate more nanoparticles [108, 109] for a higher performance, or a smaller amount of nanoparticle doping [129] can function as well as the

Table 11.1 Melting point (T_m), melting enthalpy (ΔH) and crystallinity (χ_c) of for poly (ethylene oxide) ($MW = 10^6$ g/mol)/poly(ethylene imine) ($MW = 1.2 \times 10^5$ g/mol)–LiClO₄ (PEO: PEI = 10:1) CPEs containing 0, 2, 4, 6 and 8 wt% AS-IL [129]

Content of AS-IL	T_m (°C)	ΔH_m (J/g)	χ_c (%)
a (0 wt%)	60.67	32.1	46.5
b (2 wt%)	55.23	31.7	45.8
c (4 wt%)	53.66	28.7	41.5
d (6 wt%)	51.89	27.8	40.2
e (8 wt%)	46.29	27.2	39.6

unmodified ternary CPEs. Moreover, in CPE studies with modified nanoparticles, the observation that “the sample with nanoparticle doping amount for lowest crystallinity point did not exhibit highest conductivity” [129] has not been thoroughly explained, even though the ion transport is believed to be facilitated in the amorphous state of the polymer matrix.

11.5 Quaternary Polymer Electrolytes

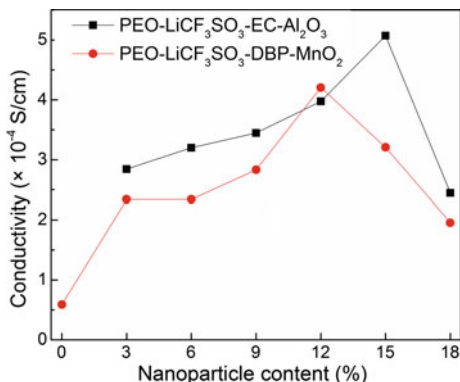
After the discussion in Sect. 11.4 concerning chemically modified nanoparticles in CPEs, we discuss here an alternative for CPE formulation, which is the physical addition of a fourth component in order to improve the performance. The advantages of this approach are the vast choice of co-additives and its ease of implementation (blending as opposed to organic/inorganic chemistry). We discuss here pseudo-quaternary systems consisting of polymer, salt, nanoparticles, and solvent. Two typical classes of the fourth CPE component are organic solvents as plasticizers and ionic liquids. These are highlighted in Sects. 11.5.1 and 11.5.2, respectively.

11.5.1 Organic Solvent Additives

Organic solvent-based electrolytes have been traditionally employed to obtain a high ionic conductivity such as 10^{-2} S/cm [16, 131, 132]. Organic solvents have also been added to polymer electrolytes to produce gel polymer electrolytes (GPE) [133–135]. Given the organic solvent contribution to a high conductivity, organic solvents have been employed as co-additives together with nanoparticles in CPEs. This is a popular approach due to a wide range of additive choices. Selected examples of such quaternary CPEs are discussed in this section.

Conductivity results of plasticized PEO–16 wt% LiCF₃SO₃–20 wt% EC incorporating 3–18 wt% of Al₂O₃ ($d = 11.8$ nm) [136] are shown in Fig. 11.9.

Fig. 11.9 Conductivity for PEO–LiCF₃SO₃–EC CPEs at different wt% Al₂O₃, and for PEO–LiCF₃SO₃–DBP CPEs as a function of MnO₂ content at room temperature (Data from Johan et al. [136, 137])



The addition of 15 wt% Al₂O₃ fillers maximized the ionic conductivity to 5.07×10^{-4} S/cm. For plasticized PEO (600,000 g/mol)–LiCF₃SO₃ (LiTf, Lithium triflate)–dibutyl phthalate (DBP) (20 wt%) incorporating MnO₂ ($d = 12$ – 15 nm), a maximum conductivity of 4.3×10^{-4} S/cm was achieved at 12 wt% MnO₂ [137]. Noticeably, the organic solvent-plasticized CPEs tend to accommodate more nanoparticles for optimized ionic conductivity.

The ionic conductivity of systems comprising PEO (4×10^6 g/mol)–LiCF₃SO₃ (EO:Li⁺ = 9)–EC–Al₂O₃ (5.8 nm pore size, 150 mesh, neutral) is shown in Fig. 11.10 [138]. The observed conductivity enhancement originated from the structural modifications caused by the plasticizer and the nanoparticles. A sample consisting of PEO (4×10^6 g/mol)–LiCF₃SO₃ (EO:Li⁺ = 9)–50 wt% EC–15 wt% Al₂O₃ (5.8 nm pore size, 150 mesh, neutral) exhibited the lowest T_g and T_m values together with the highest conductivity. However, in the case where EC was not added, the conductivity versus nanoparticle amount revealed that the highest conductivity occurred at 13 wt% Al₂O₃, which is lower than that at 15 wt% observed in the presence of EC. Compared to results from other ternary systems which usually present optimal conductivity at 10 wt% nanoparticle doping [92, 106, 107], the plasticized polymer electrolytes can accommodate higher amounts of nano-additives, with the assistance of organic solvent.

In parallel with the conductivity results, the thermal properties of polymer electrolytes incorporating co-additives reflect the conductivity trend to some extent, and thus can be employed to explain the conductivity changes. The T_g and T_m values for the binary PEO (4×10^6 g/mol)–LiCF₃SO₃ (Lithium triflate, LiTf, EO:Li⁺ = 9) electrolytes were -44 and 58 °C, respectively [138]. Both T_g and T_m decreased with the addition of either Al₂O₃ filler or EC plasticizer. A quaternary system containing both nanoparticle and plasticizer further brought down both T_m and T_g as shown by samples 1–6 in Table 11.2 [138]. Follow-up work with TiO₂ (particle size not provided [90]) together with EC plasticizer added to the same binary system of PEO (4×10^6 g/mol)–Lithium triflate (LiTf) (EO:Li⁺ = 9) exhibited a similar trend of T_m and T_g drop [90]. For samples 7–9 in Table 11.2, the activation energy (E_a) decreased from 120.6 to 78.8 kJ/mol with the addition of 10

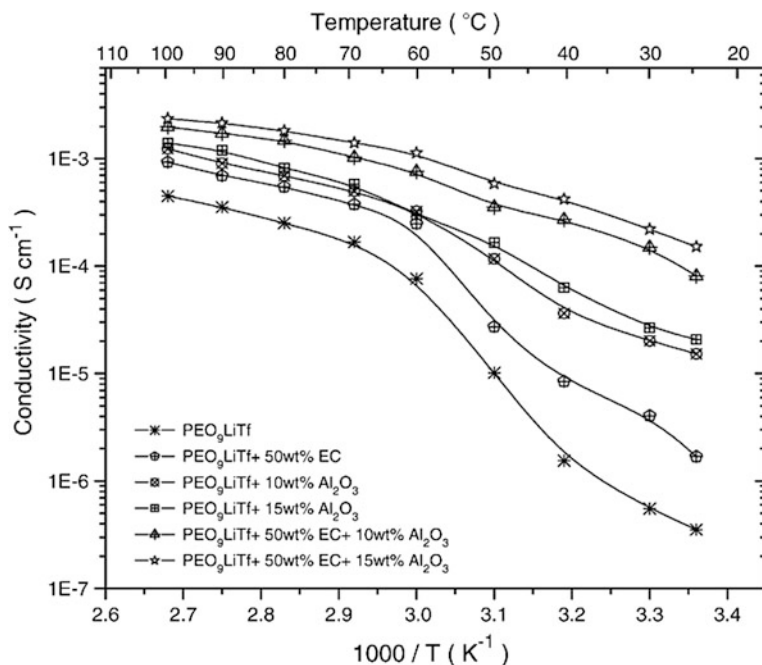


Fig. 11.10 Variation of the ionic conductivity with inverse temperature for the composite polymer electrolyte systems: PEO–LiTf, PEO–LiTf–50 wt% EC, PEO–LiTf–10 wt% Al_2O_3 , PEO–LiTf–15 wt% Al_2O_3 , PEO–LiTf–50 wt% EC–10 wt% Al_2O_3 , PEO–LiTf–50 wt% EC–15 wt% Al_2O_3 . EO:Li⁺ = 9 for all samples (Reproduced from Ref. [138] with kind permission of © 2007 Elsevier)

wt% TiO_2 , and further decreased to 57.5 kJ/mol with addition of both 10 wt% TiO_2 and 50 wt% EC at temperatures below 60 °C. This activation energy decrease suggested an improved mobility of ions within the polymer matrix, and hence increased conductivity. Whereas at temperatures above 60 °C, nearly equal E_a values were obtained for binary, ternary, and quaternary samples [138]. The conductivity increase could be explained by the improved ion mobility in the melted matrix above T_m , which overwhelmed the effect from added nanoparticles or plasticizer. For the plasticized CPE of PEO–LiTf (EO:Li⁺ = 9)–50 wt% EC, addition of 15 wt% Al_2O_3 exhibited the lowest T_g and T_m (T_g decreased to –56 °C and T_m to 49 °C, respectively). The doping amount of 15 wt% differs from that reported to give optimal thermal property in ternary CPEs (without EC) at 10 wt% nanoparticles [92, 106, 107]. The difference originated from the plasticizing effect to accommodate more nanoparticles before aggregation would take place. As a result, the optimal content of nanoparticle doping increased from 10 to 15 wt%.

A similar trend was obtained for a system of the same components but with different formulation for optimal properties [136]. PEO (MW not provided)–16 wt% LiCF_3SO_3 –20 wt% EC–15 wt% Al_2O_3 ($d = 11.8$ nm) gave the lowest T_g and T_m

Table 11.2 Crystallite melting temperatures (T_m), glass transition temperatures (T_g), and conductivity of different PEO (4×10^6 g/mol)–LiCF₃SO₃ (LiTf: Lithium triflate, EO:Li⁺ = 9)–Al₂O₃/TiO₂ samples from [138] and [90]

Sample number	Polymer electrolyte	T_m (°C)	T_g (°C)	σ at 25 °C (Scm ⁻¹)
1	^a (PEO) ₉ LiTf	58	-44	3.5×10^{-7}
2	^a (PEO) ₉ LiTf-50 wt% EC ^a	57	-48	1.6×10^{-6}
3	^a (PEO) ₉ LiTf-10 wt% Al ₂ O ₃	54	-49	1.5×10^{-5}
4	^a (PEO) ₉ LiTf-15 wt% Al ₂ O ₃	51	-50	2.1×10^{-5}
5	^a (PEO) ₉ LiTf-50 wt% EC-10 wt% Al ₂ O ₃	50	-53	8.2×10^{-5}
6	^a (PEO) ₉ LiTf-50 wt% EC-15 wt% Al ₂ O ₃	49	-56	1.5×10^{-4}
7	^b (PEO) ₉ LiTf	64	-39	^c 1.4×10^{-6}
8	^b (PEO) ₉ LiTf-10 wt% TiO ₂	60	-46	^c 4.9×10^{-5}
9	^b (PEO) ₉ LiTf-10 wt% TiO ₂ -50 wt% EC	50	-50	^c 1.6×10^{-4}

^aResults from Pitawala's work [138]^bResults from Vignarooban's work [90]^c: σ at 30 °C

values, resulting from increased amorphous percentage and segmental flexibility caused by the EC plasticizer and the nano-filler [139–141]. However, the PEO (600,000 g/mol)–LiCF₃SO₃–dibutyl phthalate (DBP)–MnO₂ (12–15 nm) CPE exhibited a different change of T_g . As related to the polymer chain segmental movement, T_g increased marginally to -70 °C when MnO₂ was added to the plasticized system ($T_g = -74$ °C) and to the binary system ($T_g = -71$ °C).

From a comparison of these quaternary CPE systems with binary polymer + salt electrolytes and ternary CPE systems, we can see that for binary systems, T_g increased from neat PEO to binary PEO–Li⁺ mixtures due to the transient crosslink formation between Li⁺ and ether oxygens [98, 142, 143]. In ternary CPEs, nanoparticles tended to further decrease T_g , by different extent as different types of nanoparticles were used, while this is not always the case for quaternary systems. Organic solvent and nanoparticle co-additives make it more complicated to draw a general rule to predict property change upon additive incorporation. Further knowledge [144] on this promising direction would be desirable.

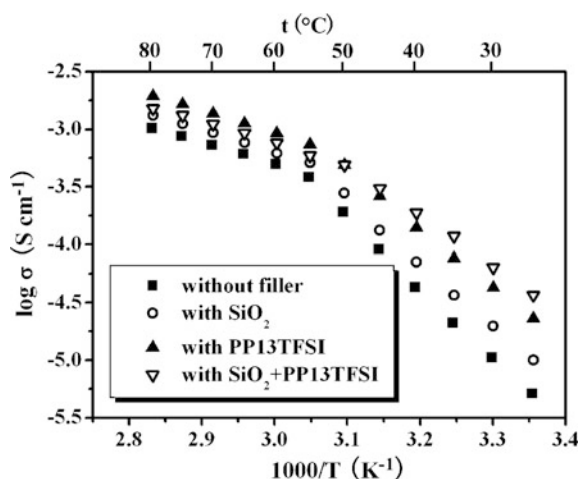
11.5.2 Ionic Liquid Additives

Ionic liquids have been extensively studied as additives for polymer electrolytes due to the unique properties of low-melting temperature and low vapor pressure [122, 145–147]. Reviews and research papers on ionic liquids as additives for polymer electrolytes have been published [148–151]. Here, we focus on physical co-doping of ionic liquids together with nanoparticles in CPEs.

Ternary systems of PEO–lithium bis (trifluoromethanesulfonyl) imide (LiTFSI, EO:Li⁺ = 18)–10 wt%–nano-sized SiO₂ [152] and PEO–LiTFSI (EO:Li⁺ = 18)–*N*-methyl-*N*-propylpiperidinium bis(trifluoromethanesulfonyl) imide (1.44 PP₁₃TFSI) have been reported [153]. In the discussion of quaternary systems of this subsection, nanoparticles and ionic liquids are doped together for the system of PEO (6 × 10⁵ g/mol)–LiTFSI (EO:Li⁺ = 18)–10 wt% SiO₂ (*d* = 50 nm)–PP₁₃TFSI (Li⁺/PP₁₃⁺ = 1:1.44) [154]. The conductivity exhibited an Arrhenius behavior as shown in Fig. 11.11. Conductivity enhancement in the melt state (*T* > *T*_m) by co-doping is not obvious, but at temperatures below the melting point (*T* < *T*_m), the enhancement is significant as explained by the activation energy decrease. From the Arrhenius plots of conductivity, with the addition to PEO₁₈LiTFSI of (1) nano-SiO₂, (2) PP₁₃TFSI, or (3) both nano-SiO₂ and PP₁₃TFSI, the activation energy (*E*_a) decreased from 115.3 kJ/mol for the binary PEO₁₈LiTFSI to (1) 105.0 kJ/mol, (2) 97.6 kJ/mol, and (3) 82.9 kJ/mol, respectively. The lower *E*_a value implies a higher mobility of the lithium cations within the polymer matrix; the lowest *E*_a and highest σ values were achieved by the co-doped sample at the low-temperature region. In contrast, in the high-temperature region, *E*_a remained almost constant for all samples (35.1–37.2 kJ/mol) [154].

In closing Sect. 11.5, the physical modification of ternary CPEs can be summarized as “tuning the recipe” of binary polymer electrolytes (polymer + Li⁺) by adding more ingredients to modulate interactions among nanoparticles, PEO (ether oxygens), and lithium ions within the system, and to affect properties such as crystallinity, glass transition temperature, and dielectric. The property changes favor an improvement of the ionic conductivity performance.

Fig. 11.11 Temperature dependence of the conductivity for PEO–LiTFSI, PEO–LiTFSI–SiO₂, PEO–LiTFSI–PP₁₃TFSI and PEO–LiTFSI–SiO₂–PP₁₃TFSI (EO:Li⁺ = 18 for all samples) (Reproduced from Ref. [154] with kind permission of © 2011 Elsevier)



11.6 Summary and Outlook

Polymer electrolytes typically based on poly(ethylene oxide) and a lithium salt are being considered to improve the mechanical strength, thermal stability, and safety over traditional organic solvent-based electrolytes. The development of polymer electrolytes involves the simultaneous improvement of desirable properties for lithium-ion batteries.

For binary systems (polymer + lithium salt) [21], given the knowledge of Li^+ motion mechanism in PEO-based polymer electrolytes, controlling the polymer architecture and morphology are effective methods to improve the polymer electrolyte performance. However, it is difficult in binary polymer + salt systems to meet the performance required in practical applications. A breakthrough occurred when nano-additives were incorporated into binary systems for conductivity improvement [24–27]. This conductivity improvement can be explained by functions affected by nanoparticle: creating more amorphous domains, promoting lithium salt dissolution. Generally, samples with 5–12 wt% nanoparticle (depending on the type of additive and its surface, typically at 10 wt%) and molar ratio $\text{EO}:\text{Li}^+ = 6\text{--}20$ (typically at 8–10) yield the optimal ionic conductivity together with lowest degree of polymer crystallinity (χ_c), decreased glass transition temperature (T_g) and melting temperature (T_m), and improved mechanical strength [92, 103, 106, 155].

However, CPEs also suffer from possible nanoparticle agglomeration within the polymer matrix. This can limit the performance enhancement due to nanoparticles. The room temperature ionic conductivity, a critical performance indicator of ternary CPEs, remains below the desired level of 10^{-3} S/cm. In order to further improve the CPE performance, modified CPEs (PEO + salt +-modified nanoparticle and PEO + salt + nanoparticle + solvent) are being considered aiming to tune pre-existing interactions within polymer matrix.

Section 11.4 discusses nanoparticles that are chemically modified for an improved compatibility within CPEs. POSS–PEO₈ can be accommodated up to 30 wt% in high molecular weight polymer matrix due to the improved compatibility conferred by the PEO end groups. The conductivity improvement ranged from a few times in temperatures above T_m to almost two orders of magnitude in the low-temperature range. However, the conductivity dropped marginally when adding 10 and 20 wt% [110]. PEO–silica into PEGDME (200 g/mol) matrix due to the increased viscosity. Incorporation of PEO–silica in high molecular weight polymer electrolyte has not been reported yet; as for non-polymer modification of silica, the best conductivity that can be achieved in this case is a little higher than 10^{-5} S/cm at room temperature, which is less effective than that reported for the quaternary (polymer + salt + nanoparticle + solvent) polymer electrolytes discussed in Sect. 11.5.

Section 11.5 discusses the doping of CPEs with a fourth component in order to further modulate interactions. In the case of nanoparticle doping with an ionic liquid, the optimal room temperature conductivity can be in the range $10^{-4.5}\text{--}10^{-4}$ S/cm. This approach did not always increase the conductivity over the whole temperature

range studied when compared to ternary systems of polymer + Li⁺ + ionic liquid. In comparison, co-doping with nanoparticles and organic solvents for CPEs led to an obvious degree of crystallinity drop and marginal T_g and T_m decreases compared to ternary plasticized system (polymer + Li⁺ + organic plasticizer). The conductivity enhancement is less than one order of magnitude (about 2–8 times) and presented an optimal conductivity a little lower than 10^{-4} S/cm at room temperature. It becomes apparent from the above that for quaternary polymer electrolytes, a level of 10^{-4} S/cm room temperature ionic conductivity is still difficult to achieve, and co-doping has shown limited contribution toward conductivity enhancement.

The research in CPEs is experiencing a bottleneck in that the highest ionic conductivity reported for solid-state CPEs just got close to 10^{-3} S/cm at room temperature [156–158], still not high enough to compete effectively with traditional organic solvent-based electrolytes. Future research in this field could fall into two broad directions. The first direction encompasses three-dimensional nano-scale ordered structure fabrication [105], such as ion tunnels [159] or ion paths [160], to facilitate ion conduction. Grafting side chains [161, 162] or a block of different chemistry [163–165] on the PEO polymer backbone can also be viewed as a nano-scale fabrication if further ordered structure can be obtained. The second direction is to adjust the CPE composition, with addition of certain other additives conferring special functions [90, 92, 137, 138, 166]. Sections 11.4 and 11.5 exemplify the current status of these two directions. The discussion in this chapter of various formulation strategies for electrolyte performance enhancement is intended to further stimulate the design of novel CPEs.

Acknowledgements This work has been supported by the American Chemical Society Petroleum Research Fund (Grant 51623-ND7).

References

1. Scrosati B (1995) Battery technology-challenge of portable power. *Nature* 373(6515):557–558
2. Tarascon JM, Armand M (2001) Issues and challenges facing rechargeable lithium batteries. *Nature* 414(6861):359–367
3. Wakihara M (2001) Recent developments in lithium ion batteries. *Mater Sci Eng, R* 33(4):109–134
4. Yoo HD, Markevich E, Salitra G et al (2014) On the challenge of developing advanced technologies for electrochemical energy storage and conversion. *Mater Today* 17(3):110–121
5. Winter M, Brodd RJ (2004) What are batteries, fuel cells, and supercapacitors. *Chem Rev* 104(10):4245–4269
6. Antunes RA, de Oliveira MCL, Ett G et al (2011) Carbon materials in composite bipolar plates for polymer electrolyte membrane fuel cells a review of the main challenges to improve electrical performance. *J Power Sources* 196(6):2945–2961
7. Frederick T, Wagner BL, Mathias MF (2010) Electrochemistry and the future of the automobile. *J Phys Chem Lett* 1:2204–2219

8. Simon P, Gogotsi Y (2008) Materials for electrochemical capacitors. *Nat Mater* 7(11):845–854
9. Nitta N, Wu F, Lee JT et al (2015) Li-ion battery materials: present and future. *Mater Today* 18(5):252–264
10. Palacin MR (2009) Recent advances in rechargeable battery materials: a chemist's perspective. *Chem Soc Rev* 38(9):2565–2575
11. Chen J, Cheng F (2009) Combination of lightweight elements and nanostructured materials for batteries. *Acc Chem Res* 42(6):713–723
12. Xu K (2014) Electrolytes and interphases in Li-ion batteries and beyond. *Chem Rev* 114(23):11503–11618
13. Scrosati B, Vincent CA (2000) Polymer electrolytes the key to lithium polymer batteries. *MRS Bull* 25(3):28–30
14. Kalhoff J, Eshetu GG, Bresser D et al (2015) Safer electrolytes for lithium-ion batteries: state of the art and perspectives. *ChemSusChem* 8(13):2154–2175
15. Cheng FY, Liang J, Tao ZL et al (2011) Functional materials for rechargeable batteries. *Adv Mater* 23(15):1695–1715
16. Xu K (2004) Nonaqueous liquid electrolytes for lithium-based rechargeable batteries. *Chem Rev* 104(10):4303–4417
17. Quartarone E, Mustarelli P (2011) Electrolytes for solid-state lithium rechargeable batteries: recent advances and perspectives. *Chem Soc Rev* 40(5):2525–2540
18. He Z, Alexandridis P (2017) Ionic liquid and nanoparticle hybrid systems: emerging applications. *Adv Colloid Interface Sci*. doi:10.1016/j.cis.2016.08.004
19. He ZQ, Alexandridis P (2015) Nanoparticles in ionic liquids: interactions and organization. *Phys Chem Chem Phys* 17(28):18238–18261
20. Berthier C, Gorecki W, Minier M et al (1983) Microscopic investigation of ionic-conductivity in alkali-metal salts poly(ethylene oxide) adducts. *Solid State Ionics* 11(1):91–95
21. Armand MB (1986) Polymer electrolytes. *Annu Rev Mater Sci* 16:245–261
22. Fenton DE, Parker JM, Wright PV (1973) Complexes of alkali-metal ions with poly(ethylene oxide). *Polymer* 14(11):589
23. Wang W, Alexandridis P (2016) Composite polymer electrolytes: nanoparticles affect polymers structure and properties. *Polymers* 8(11):387
24. Florjanczyk Z, Marcinek M, Wieczorek W et al (2004) Review of PEO based composite polymer electrolytes. *Pol J Chem* 78(9):1279–1304
25. Quartarone E, Mustarelli P, Magistris A (1998) PEO-based composite polymer electrolytes. *Solid State Ionics* 110(1–2):1–14
26. Jung S (2009) Fillers for solid-state polymer electrolytes. *Bull Korean Chem Soc* 30(10):2355–2361
27. Stephan AM, Nahm KS (2006) Review on composite polymer electrolytes for lithium batteries. *Polymer* 47(16):5952–5964
28. Baldwin RS, Bennett WR (2007) The NASA “PERS” program: solid polymer electrolyte development for advanced lithium-based batteries
29. Borodin O, Smith GD (2006) Mechanism of ion transport in amorphous poly(ethylene oxide)/LiTFSI from molecular dynamics simulations. *Macromolecules* 39(4):1620–1629
30. Borodin O, Smith GD (2007) Molecular dynamics simulations of comb-branched poly(epoxide ether)-based polymer electrolytes. *Macromolecules* 40(4):1252–1258
31. Borodin O, Smith GD, Bandyopadhyaya R et al (2004) Molecular dynamics study of nanocomposite polymer electrolyte based on poly(ethylene oxide)/LiBF₄. *Modell Simul Mater Sci En* 12(3):S73–S89
32. Brandell D, Priimägi P, Kasemägi H et al (2011) Branched polyethylene/poly(ethylene oxide) as a host matrix for Li-ion battery electrolytes a molecular dynamics study. *Electrochim Acta* 57:228–236

33. Ferreira B, Mullerplathe F, Bernardes A et al (2002) A comparison of Li^+ transport in dimethoxyethane, poly(ethylene oxide) and poly(tetramethylene oxide) by molecular dynamics simulations. *Solid State Ionics* 147(3–4):361–366
34. Hektor A, Klintonberg MK, Aabloo A et al (2002) Molecular dynamics simulation of the effect of a side chain on the dynamics of the amorphous LiPF_6 -PEO system. *J Mater Chem* 13(2):214–218
35. Karo J, Brandell D (2009) A molecular dynamics study of the influence of side-chain length and spacing on lithium mobility in non-crystalline LiPF_6 -PEO_x; x = 10 and 30. *Solid State Ionics* 180(23–25):1272–1284
36. Maitra A, Heuer A (2007) Understanding segmental dynamics in polymer electrolytes: a computer study. *Macromol Chem Phys* 208(19–20):2215–2221
37. Müller-Plathe F, van Gunsteren WF (1995) Computer simulation of a polymer electrolyte: lithium iodide in amorphous poly(ethylene oxide). *J Chem Phys* 103(11):4745–4756
38. Siqueira LJA, Ribeiro MCC (2005) Molecular dynamics simulation of the polymer electrolyte poly(ethylene oxide)/ LiClO_4 structural properties. *J Chem Phys* 122(19):194911
39. Siqueira LJA, Ribeiro MCC (2006) Molecular dynamics simulation of the polymer electrolyte poly(ethylene oxide)/ LiClO_4 II dynamical properties. *J Chem Phys* 125(21):214903
40. Snyder J (2002) Polymer electrolytes and polyelectrolytes: Monte Carlo simulations of thermal effects on conduction. *Solid State Ionics* 147(3–4):249–257
41. Diddens D, Heuer A, Borodin O (2010) Understanding the lithium transport within a rouse-based model for a PEO/LiTFSI polymer electrolyte. *Macromolecules* 43(4):2028–2036
42. Sutjianto A, Curtiss LA (1998) Li^+ -diglyme complexes: barriers to lithium cation migration. *J Phys Chem A* 102(6):968–974
43. Borodin O, Smith GD (2007) Li^+ transport mechanism in oligo(ethylene oxide)s compared to carbonates. *J Solution Chem* 36(6):803–813
44. Li Z, Smith GD, Bedrov D (2012) Li^+ Solvation and transport properties in ionic liquid/lithium salt mixtures: a molecular dynamics simulation study. *J Phys Chem B* 116(42):12801–12809
45. Borodin O, Smith GD (2006) Development of many-body polarizable force fields for Li-battery applications. *J Phys Chem B* 110(12):6293–6299
46. Hayamizu K, Akiba E, Bando T et al (2002) H-1, Li-7, and F-19 nuclear magnetic resonance and ionic conductivity studies for liquid electrolytes composed of glymes and polyethenoglycol dimethyl ethers of $\text{CH}_3\text{O}(\text{CH}_2\text{CH}_2\text{O})_n\text{CH}_3$ ($n = 3$ –50) doped with $\text{Li}(\text{SO}_2\text{CF}_3)_2$. *J Chem Phys* 117(12):5929–5939
47. Edman L, Ferry A, Orädd G (2002) Analysis of diffusion in a solid polymer electrolyte in the context of a phase-separated system. *Phys Rev E* 65(4):042803
48. Lascaud S (1994) Phase diagrams and conductivity behavior of poly(ethylene oxide)-molten salt rubbery electrolytes. *Macromol* 27(25):7469–7477
49. Voegelé A, Deimedé V, Paloukis F et al (2014) Synthesis and properties of aromatic polyethers containing poly(ethylene oxide) side chains as polymer electrolytes for lithium ion batteries. *Mater Chem Phys* 148(1–2):57–66
50. Buriez O, Han YB, Hou J et al (2000) Performance limitations of polymer electrolytes based on ethylene oxide polymers. *J Power Sources* 89(2):149–155
51. Kerr JB, Sloop SE, Liu G et al (2002) From molecular models to system analysis for lithium battery electrolytes. *J Power Sources* 110(2):389–400
52. Smith GD, Borodin O (2012) Lithium battery electrolyte stability and performance from molecular modeling and simulations. In: *Batteries for sustainability*. Springer Science Business Media, New York, pp 195–237
53. Wu H, Wick CD (2010) Computational investigation on the role of plasticizers on ion conductivity in poly(ethylene oxide) LiTFSI electrolytes. *Macromolecules* 43(7):3502–3510
54. Meziane R, Bonnet JP, Courty M et al (2011) Single-ion polymer electrolytes based on a delocalized polyanion for lithium batteries. *Electrochim Acta* 57:14–19

55. Inceoglu S, Rojas AA, Devaux D et al (2014) Morphology-conductivity relationship of single-ion-conducting block copolymer electrolytes for lithium batteries. *ACS Macro Letters* 3(6):510–514
56. Amine K, Wang Q, Vissers DR et al (2006) Novel silane compounds as electrolyte solvents for Li-ion batteries. *Electrochem Commun* 8(3):429–433
57. Nakahara H, Tanaka M, Yoon S-Y et al (2006) Electrochemical and thermal stability of a siloxane-based electrolyte on a lithium transition metal oxide cathode. *J Power Sources* 160(1):645–650
58. Zhang Z, Dong J, West R et al (2010) Oligo(ethylene glycol)-functionalized disiloxanes as electrolytes for lithium-ion batteries. *J Power Sources* 195(18):6062–6068
59. Rossi NAA, West R (2009) Silicon-containing liquid polymer electrolytes for application in lithium ion batteries. *Polym Int* 58(3):267–272
60. Karatas Y, Kaskhedikar N, Burjanadze M et al (2006) Synthesis of cross-linked comb polysiloxane for polymer electrolyte membranes. *Macromol Chem Phys* 207(4):419–425
61. Kunze M, Karatas Y, Wiemhöfer H-D et al (2010) Activation of transport and local dynamics in polysiloxane-based salt-in-polymer electrolytes: a multinuclear NMR study. *Phys Chem Chem Phys* 12(25):6844–6851
62. Zhang Z, Jin J, Bautista F et al (2004) Ion conductive characteristics of cross-linked network polysiloxane-based solid polymer electrolytes. *Solid State Ionics* 170(3–4):233–238
63. Zhang Z, Lyons LJ, West R et al (2007) Synthesis and ionic conductivity of mixed substituted polysiloxanes with oligoethyleneoxy and cyclic carbonate substituents. *Silicon Chem* 3(5):259–266
64. Ruzette AVG, Soo PP, Sadoway DR et al (2001) Melt-formable block copolymer electrolytes for lithium rechargeable batteries. *J Electrochem Soc* 148(6):A537–A543
65. Chen J, Frisbie CD, Bates FS (2009) Lithium perchlorate-doped poly(styrene-*b*-ethylene oxide-*b*-styrene) lamellae-forming triblock copolymer as high capacitance, smooth, thin film dielectric. *J Phys Chem C* 113(10):3903–3908
66. Gomez ED, Panday A, Feng EH et al (2009) Effect of ion distribution on conductivity of block copolymer electrolytes. *Nano Lett* 9(3):1212–1216
67. Young WS, Epps TH (2009) Salt doping in peo-containing block copolymers: counterion and concentration effects. *Macromolecules* 42(7):2672–2678
68. Hallinan DT, Balsara NP (2013) Polymer electrolytes. *Annu Rev Mater Res* 43(1):503–525
69. Young WS, Kuan WF, Epps TH (2014) Block copolymer electrolytes for rechargeable lithium batteries. *J Polym Sci Pol Phys* 52(1):1–16
70. Spontak RJ, Alexandridis P (1999) Advances in self-ordering macromolecules and nanostructure design. *Curr Opin Colloid Interface Sci* 4(2):140–146
71. Schmidt G, Richtering W, Lindner P et al (1998) Shear orientation of a hexagonal lyotropic triblock copolymer phase as probed by flow birefringence and small-angle light and neutron scattering. *Macromolecules* 31(7):2293–2298
72. Zipfel J, Berghausen J, Schmidt G et al (2002) Influence of shear on solvated amphiphilic block copolymers with lamellar morphology. *Macromolecules* 35(10):4064–4074
73. Ayandele E, Sarkar B, Alexandridis P (2012) Polyhedral oligomeric silsesquioxane (POSS)-containing polymer nanocomposites. *Nanomaterials* 2(4):445–475
74. Edwards EW, Stoykovich MP, Müller M et al (2005) Mechanism and kinetics of ordering in diblock copolymer thin films on chemically nanopatterned substrates. *J Polym Sci Pol Phys* 43(23):3444–3459
75. Golodnitsky D, Peled E (2000) Stretching-induced conductivity enhancement of LiI(PEO)-polymer electrolyte. *Electrochim Acta* 45(8–9):1431–1436
76. Hu H, Gopinadhan M, Osuji CO (2014) Directed self-assembly of block copolymers: a tutorial review of strategies for enabling nanotechnology with soft matter. *Soft Matter* 10(22):3867
77. Kim JK, Lee JI, Lee DH (2008) Self-assembled block copolymers: bulk to thin film. *Macromol Res* 16(4):267–292

78. Kovarsky R, Golodnitsky D, Peled E et al (2011) Conductivity enhancement induced by casting of polymer electrolytes under a magnetic field. *Electrochim Acta* 57:27–35
79. Majewski PW, Gopinadhan M, Jang W-S et al (2010) Anisotropic ionic conductivity in block copolymer membranes by magnetic field alignment. *J Am Chem Soc* 132(49):17516–17522
80. Marencic AP, Register RA (2010) Controlling order in block copolymer thin films for nanopatterning applications. *Annu Rev Chem Biomol Eng* 1(1):277–297
81. Tong Q, Sibener SJ (2014) Electric-field-induced control and switching of block copolymer domain orientations in nanoconfined channel architectures. *J Phys Chem C* 118(25):13752–13756
82. Li J, Kamata K, Komura M et al (2007) Anisotropic ion conductivity in liquid crystalline diblock copolymer membranes with perpendicularly oriented PEO cylindrical domains. *Macromol* 40(23):8125–8128
83. Sarkar B, Alexandridis P (2015) Block copolymer-nanoparticle composites: structure, functional properties, and processing. *Prog Polym Sci* 40:33–62
84. Young WS, Epps TH (2012) Ionic conductivities of block copolymer electrolytes with various conducting pathways: sample preparation and processing considerations. *Macromol* 45(11):4689–4697
85. Mullin SA, Teran AA, Yuan R et al (2013) Effect of thermal history on the ionic conductivity of block copolymer electrolytes. *J Polym Sci Pol Phys* 51(12):927–934
86. Chintapalli M, Chen XC, Thelen JL et al (2014) Effect of grain size on the ionic conductivity of a block copolymer electrolyte. *Macromol* 47(15):5424–5431
87. Weber RL, Ye Y, Schmitt AL et al (2011) Effect of nanoscale morphology on the conductivity of polymerized ionic liquid block copolymers. *Macromolecules* 44(14):5727–5735
88. Williams ML, Landel RF, Ferry JD (1955) The temperature dependence of relaxation mechanisms in amorphous polymers and other glass-forming liquids. *J Am Chem Soc* 77:3701–3707
89. Rietman EA, Kaplan ML, Cava RJ (1985) Lithium ion-poly (ethylene-oxide) complexes. 1. Effect of anion on conductivity. *Solid State Ionics* 17(1):67–73
90. Vignarooban K, Dissanayake MAKL, Albinsson I et al (2014) Effect of TiO₂ nano-filler and ec plasticizer on electrical and thermal properties of poly(ethylene oxide) (PEO) based solid polymer electrolytes. *Solid State Ionics* 266:25–28
91. Zugmann S, Gores H (2014) Transference numbers of ions in electrolytes. In: Kreysa G, Ota K-I, Savinell R (eds) *Encyclopedia of applied electrochemistry*. Springer, New York, pp 2086–2091
92. Wang XL, Mei A, Li M et al (2007) Polymer composite electrolytes containing ionically active mesoporous SiO₂ particles. *J Appl Phys* 102(5):054907
93. Gorecki W, Andreani R, Berthier C et al (1986) NMR, DSC, and conductivity study of a poly(ethylene oxide) complex electrolyte: PEO(LiClO₄)_n. *Solid State Ionics* 18–9:295–299
94. McLin MG, Angell CA (1996) Probe ion diffusivity measurements in salt-in-polymer electrolytes: stokes radii and the transport number problem. *J Phys Chem* 100(4):1181–1188
95. Abbrent S, Greenbaum S (2013) Recent progress in NMR spectroscopy of polymer electrolytes for lithium batteries. *Curr Opin Colloid Interface Sci* 18(3):228–244
96. Volkov VI, Marinin AA (2013) NMR methods for studying ion and molecular transport in polymer electrolytes. *Russ Chem Rev* 82(3):248–272
97. Golodnitsky D, Ardel G, Peled E (2002) Ion-transport phenomena in concentrated PEO-based composite polymer electrolytes. *Solid State Ionics* 147(1–2):141–155
98. Ciosek M, Sannier L, Siekierski M et al (2007) Ion transport phenomena in polymeric electrolytes. *Electrochim Acta* 53(4):1409–1416
99. Croce F, Persi L, Scrosati B et al (2001) Role of the ceramic fillers in enhancing the transport properties of composite polymer electrolytes. *Electrochim Acta* 46(16):2457–2461

100. Wang XL, Mei A, Li M et al (2006) Effect of silane-functionalized mesoporous silica SBA-15 on performance of PEO-based composite polymer electrolytes. *Solid State Ionics* 177(15–16):1287–1291
101. Bandara LRAK, Dissanayake MAKL, Furlani M et al (2000) Broad band dielectric behavior of plasticized PEO-based solid polymer electrolytes. *Ionics* 6(3–4):239–247
102. Fan L (2003) Effect of modified SiO₂ on the properties of PEO-based polymer electrolytes. *Solid State Ionics* 164(1–2):81–86
103. Croce F, Appetecchi GB, Persi L et al (1998) Nanocomposite polymer electrolytes for lithium batteries. *Nature* 394(6692):456–458
104. Appetecchi GB, Carewska M, Alessandrini F et al (2000) Characterization of PEO-based composite cathodes morphological thermal, mechanical, and electrical properties. *J Electrochem Soc* 147(2):451–459
105. Tang CY, Hackenberg K, Fu Q et al (2012) High ion conducting polymer nanocomposite electrolytes using hybrid nanofillers. *Nano Lett* 12(3):1152–1156
106. Karmakar A, Ghosh A (2011) Poly ethylene oxide (PEO)-LiI polymer electrolytes embedded with CdO nanoparticles. *J Nanopart Res* 13(7):2989–2996
107. Fan LZ, Dang ZM, Wei GD et al (2003) Effect of nanosized ZnO on the electrical properties of (PEO)₁₆-LiClO₄ electrolytes. *Mater Sci Eng, B* 99(1–3):340–343
108. Zhang HJ, Kulkarni S, Wunder SL (2007) Blends of POSS-PEO(n = 4)₈ and high molecular weight poly(ethylene oxide) as solid polymer electrolytes for lithium batteries. *J Phys Chem B* 111(14):3583–3590
109. Zhang HJ, Kulkarni S, Wunder SL (2006) Polyethylene glycol functionalized polyoctahedral silsesquioxanes as electrolytes for lithium batteries. *J Electrochem Soc* 153(2):A239–A248
110. Fan J, Raghavan SR, Yu XY et al (1998) Composite polymer electrolytes using surface-modified fumed silicas: conductivity and rheology. *Solid State Ionics* 111(1–2):117–123
111. Cordes DB, Lickiss PD, Rataboul F (2010) Recent developments in the chemistry of cubic polyhedral oligosilsesquioxanes. *Chem Rev* 110(4):2081–2173
112. Jung G-Y, Choi JH, Lee JK (2015) Thermal behavior and ion conductivity of polyethylene oxide/polyhedral oligomeric silsesquioxane nanocomposite electrolytes. *Adv Polym Technol* 34(3):21–49
113. Kim D-G, Shim J, Lee JH et al (2013) Preparation of solid-state composite electrolytes based on organic/inorganic hybrid star-shaped polymer and PEG-functionalized POSS for all-solid-state lithium battery applications. *Polymer* 54(21):5812–5820
114. Polu AR, Rhee H-W (2015) Nanocomposite solid polymer electrolytes based on poly(ethylene oxide)/POSS-PEG (n = 13.3) hybrid nanoparticles for lithium ion batteries. *J Ind Eng Chem* 31:323–329
115. Polu AR, Rhee H-W (2015) Effect of organic–inorganic hybrid nanoparticles (POSS–PEG (n = 4)) on thermal, mechanical, and electrical properties of PEO-based solid polymer electrolytes. *Adv Polym Technol* 00:21–58
116. Chinnam PR, Wunder SL (2013) Self-assembled Janus-like multi-ionic lithium salts form nano-structured solid polymer electrolytes with high ionic conductivity and Li⁺ ion transference number. *J Mater Chem A* 1(5):1731–1739
117. Chinnam PR, Wunder SL (2011) Polyoctahedral silsesquioxane-nanoparticle electrolytes for lithium batteries: POSS-lithium salts and POSS-PEGs. *Chem Mater* 23(23):5111–5121
118. Chinnam PR, Zhang HJ, Wunder SL (2015) Blends of pegylated polyoctahedralsilsesquioxanes (POSS-PEG) and methyl cellulose as solid polymer electrolytes for lithium batteries. *Electrochim Acta* 170:191–201
119. Jia Z, Yuan W, Zhao H et al (2014) Composite electrolytes comprised of poly(ethylene oxide) and silica nanoparticles with grafted poly(ethylene oxide)-containing polymers. *RSC Adv* 4(77):41087–41098
120. O'Reilly MV, Winey KI (2015) Silica nanoparticles densely grafted with PEO for ionomer plasticization. *RSC Adv* 5(25):19570–19580

121. Wetjen M, Navarra MA, Panero S et al (2013) Composite poly(ethylene oxide) electrolytes plasticized by *N*-Alkyl-*N*-butylpyrrolidinium bis(trifluoromethanesulfonyl)imide for lithium batteries. *ChemSusChem* 6(6):1037–1043
122. Park MJ, Choi I, Hong J et al (2013) Polymer electrolytes integrated with ionic liquids for future electrochemical devices. *J Appl Polym Sci* 129(5):2363–2376
123. Ketabi S, Lian K (2013) Effect of SiO₂ on conductivity and structural properties of PEO-EMIHSO₄ polymer electrolyte and enabled solid electrochemical capacitors. *Electrochim Acta* 103:174–178
124. Chaurasia SK, Singh RK, Chandra S (2013) Ion-polymer complexation and ion-pair formation in a polymer electrolyte PEO:LiPF₆ containing an ionic liquid having same anion: a Raman study. *Vib Spectrosc* 68:190–195
125. Zhang SP, Lee KH, Sun JR et al (2011) Viscoelastic properties, ionic conductivity, and materials design considerations for poly(styrene-*b*-ethylene oxide-*b*-styrene)-based ion gel electrolytes. *Macromol* 44(22):8981–8989
126. Mecerreyes D (2011) Polymeric ionic liquids: broadening the properties and applications of polyelectrolytes. *Prog Polym Sci* 36(12):1629–1648
127. Chen XJ, Li Q, Zhao J et al (2012) Ionic liquid-tethered nanoparticle/poly(ionic liquid) electrolytes for quasi-solid-state dye-sensitized solar cells. *J Power Sources* 207:216–221
128. Moganty SS, Jayaprakash N, Nugent JL et al (2010) Ionic-liquid-tethered nanoparticles: hybrid electrolytes. *Angew Chem Int Ed* 49(48):9158–9161
129. Kim J, Park DW, Park SJ et al (2013) Ion conducting properties of poly(ethylene oxide)-based electrolytes incorporating amorphous silica attached with imidazolium salts. *Res Chem Intermed* 39(3):1409–1416
130. Lee L, Kim I-J, Yang S et al (2014) Filler effect of ionic liquid attached titanium oxide on conducting property of poly(ethylene oxide)/poly(methyl methacrylate) composite electrolytes. *Am J Nanosci Nanotechnol* 14(10):8010–8013
131. Beck F, Ruetschi P (2000) Rechargeable batteries with aqueous electrolytes. *Electrochim Acta* 45(15–16):2467–2482
132. Zhang SS (2007) A review on the separators of liquid electrolyte Li-ion batteries. *J Power Sources* 164(1):351–364
133. Croce F, Gerace F, Dautzemberg G et al (1994) Synthesis and characterization of highly conducting gel electrolytes. *Electrochim Acta* 39(14):2187–2194
134. Song JY (1999) Review of gel-type polymer electrolytes for lithium-ion batteries. *J Power Sources* 77(2):183–197
135. Soni SS, Fadadu KB, Gibaud A (2012) Ionic conductivity through thermoresponsive polymer gel: ordering matters. *Langmuir* 28(1):751–756
136. Johan MR, Shy OH, Ibrahim S et al (2011) Effects of Al₂O₃ nanofiller and ec plasticizer on the ionic conductivity enhancement of solid PEO-LiCF₃SO₃ solid polymer electrolyte. *Solid State Ionics* 196(1):41–47
137. Johan MR, Ting LM (2011) Structural, thermal and electrical properties of nano manganese-composite polymer electrolytes. *Int J Electrochem Sci* 6(10):4737–4748
138. Pitawala H, Dissanayake M, Seneviratne VA (2007) Combined effect of Al₂O₃ nano-fillers and EC plasticizer on ionic conductivity enhancement in the solid polymer electrolyte (PEO)₉LiTF. *Solid State Ionics* 178(13–14):885–888
139. Leo CJ, Rao GVS, Chowdari BVR (2002) Studies on plasticized PEO-Lithium Triflate-Ceramic filler composite electrolyte system. *Solid State Ionics* 148(1–2):159–171
140. Wang YJ, Pan Y, Wang L et al (2005) Conductivity studies of plasticized PEO-Lithium Chlorate-FIC filler composite polymer electrolytes. *Mater Lett* 59(24–25):3021–3026
141. Xi JY, Qiu XP, Ma XM et al (2005) Composite polymer electrolyte doped with mesoporous silica SBA-15 for lithium polymer battery. *Solid State Ionics* 176(13–14):1249–1260
142. Bruce PG, Vincent CA (1993) Polymer electrolytes. *J Chem Soc Faraday T* 89(17):3187–3203

143. Karan NK, Pradhan DK, Thomas R et al (2008) Solid polymer electrolytes based on polyethylene oxide and lithium trifluoro-methane sulfonate (PEO-LiCF₃SO₃): ionic conductivity and dielectric relaxation. *Solid State Ionics* 179(19–20):689–696
144. Mejia A, Garcia N, Guzman J et al (2014) Thermoplastic and solid-like electrolytes with liquid-like ionic conductivity based on poly(ethylene oxide) nanocomposites. *Solid State Ionics* 261:74–80
145. Shin JH, Henderson WA, Passerini S (2003) Ionic liquids to the rescue overcoming the ionic conductivity limitations of polymer electrolytes. *Electrochem Commun* 5(12):1016–1020
146. Shin JH, Henderson WA, Passerini S (2005) PEO-based polymer electrolytes with ionic liquids and their use in lithium Metal-Polymer electrolyte batteries. *J Electrochem Soc* 152(5):A978–A983
147. Choi J, Cheruvally G, Kim Y et al (2007) Poly(ethylene oxide)-based polymer electrolyte incorporating room-temperature ionic liquid for lithium batteries. *Solid State Ionics* 178(19–20):1235–1241
148. Zhang RS, Chen YF, Montazami R (2015) Ionic liquid-doped gel polymer electrolyte for flexible lithium-ion polymer batteries. *Mater* 8(5):2735–2748
149. Zain NF, Zainal N, Mohamed NS (2015) The influences of ionic liquid to the properties of poly(ethylmethacrylate) based electrolyte. *Phys Scripta* 90(1):015702
150. Shalu, Singh VK, Singh RK (2015) Development of ion conducting polymer gel electrolyte membranes based on polymer PVdF-HFP, BMIMTFSI ionic liquid and the Li-salt with improved electrical, thermal and structural properties. *J Mater Chem C* 3(28):7305–7318
151. Shalu, Chaurasia SK, Singh RK et al (2015) Electrical, mechanical, structural, and thermal behaviors of polymeric gel electrolyte membranes of poly(vinylidene fluoride-co-hexafluoropropylene) with the ionic liquid 1-butyl 1-3-methylimidazolium tetrafluoroborate plus lithium tetrafluoroborate. *J Appl Polym Sci* 132(7):41456
152. Liu S, Imanishi N, Zhang T et al (2010) Effect of nano-silica filler in polymer electrolyte on Li dendrite formation in Li/Poly(ethylene oxide)-Li(CF₃SO₂)₂N/Li. *J Power Sources* 195(19):6847–6853
153. Liu S, Imanishi N, Zhang T et al (2010) Lithium dendrite formation in Li/poly(ethylene oxide)-Lithium bis(trifluoromethanesulfonyl)imide and *N*-methyl-*N*-propylpiperidinium bis(trifluoromethanesulfonyl)imide/Li Cells. *J Electrochem Soc* 157(10):1092–1098
154. Liu S, Wang H, Imanishi N et al (2011) Effect of co-doping nano-silica filler and *N*-methyl-*N*-propylpiperidinium bis(trifluoromethanesulfonyl)imide into polymer electrolyte on Li dendrite formation in Li/Poly(ethylene oxide)-Li(CF₃SO₂)₂N/Li. *J Power Sources* 196(18):7681–7686
155. Aihara Y, Appetecchi GB, Scrosati B et al (2002) Investigation of the ionic conduction mechanism of composite poly(ethyleneoxide) PEO-based polymer gel electrolytes including nano-size SiO₂. *Phys Chem Chem Phys* 4(14):3443–3447
156. Qi DJ, Ru HQ, Bi XG et al (2012) A novel PEO-based composite polymer electrolyte with NaAlOSiO molecular sieves powders. *Ionics* 18(3):267–273
157. Angulakshmi N, Kumar RS, Kulandainathan MA et al (2014) Composite polymer electrolytes encompassing metal organic frame works: a new strategy for all-solid-state lithium batteries. *J Phys Chem C* 118(42):24240–24247
158. Kumar RS, Raja M, Kulandainathan MA et al (2014) Metal organic framework-laden composite polymer electrolytes for efficient and durable all-solid-state-lithium batteries. *RSC Adv* 4(50):26171–26175
159. Gadjourova Z, Andreev YG, Tunstall DP et al (2001) Ionic conductivity in crystalline polymer electrolytes. *Nature* 412(6846):520–523

160. Wang Y, Li B, Ji J et al (2014) Controlled Li⁺ conduction pathway to achieve enhanced ionic conductivity in polymer electrolytes. *J Power Sources* 247:452–459
161. Li H, Zhang H, Liang ZY et al (2014) Preparation and properties of poly (vinylidene fluoride)/poly(dimethylsiloxane) graft (poly(propylene oxide)-block-poly(ethylene oxide)) blend porous separators and corresponding electrolytes. *Electrochim Acta* 116:413–420
162. Jankowsky S, Hiller MM, Wiemhoefer HD (2014) Preparation and electrochemical performance of polyphosphazene based salt-in-polymer electrolyte membranes for lithium ion batteries. *J Power Sources* 253:256–262
163. Kwon S-J, Kim D-G, Shim J et al (2014) Preparation of organic/inorganic hybrid semi-interpenetrating network polymer electrolytes based on poly(ethylene oxide-co-ethylene carbonate) for all-solid-state lithium batteries at elevated temperatures. *Polymer* 55(12):2799–2808
164. Kuo P-L, Wu C-A, Lu C-Y et al (2014) High performance of transferring lithium ion for polyacrylonitrile-interpenetrating crosslinked polyoxyethylene network as gel polymer electrolyte. *ACS Appl Mater Interface* 6(5):3156–3162
165. Huang J, Wang RY, Tong ZZ et al (2014) Influence of ionic species on the microphase separation behavior of PCL-b-PEO/Salt hybrids. *Macromol* 47(23):8359–8367
166. Bodratti AM, Sarkar B, Alexandridis P (2017) Adsorption of poly(ethylene oxide)-containing amphiphilic polymers on solid–liquid interfaces: fundamentals and applications. *Adv Colloid Interfac*. doi:[10.1016/j.cis.2016.09.003](https://doi.org/10.1016/j.cis.2016.09.003)